ation. The results have been obtained on 1,8 dichloro-10-methyl anthracene employing electron and optical microscopy, X-ray studies and differential enthalpic analysis and will be reported in detail elsewhere [4]. The essential information relating to the present discussion is contained in Fig. 1 which shows an electron micrograph of a solution-grown crystal taken with the electron beam normal to *ac* planes. The *c*-direction is indicated and often coincides with crystallite edges (AB) or cracks (CD). Diffraction contrast arises mainly from bend extinction contours, e.g. EF, which are characteristic of the electron micrographs of thin specimens. Certain faulted areas are apparent, e.g. CG, DG, which consist of bands almost parallel to ⟨103⟩ and across which the bend extinction contours are displaced. Analysis of selected-area electron diffraction patterns reveals that the structure inside and outside the faulted regions is different and that well defined orientational relationships exist between the two structures. Furthermore, the available evidence is consistent with the occurrence of a diffusionless (martensitic) transformation [5] in this material and in many respects its behaviour is similar to that exhibited by single-crystalline and bulk polyethylene [6-8]. The procedure adopted by Bevis and Crellin [9] for investigating the crystallography of shear-like processes in polyethylene is applicable to the case of 1:8 dichloro-10-methyl anthracene, but the latter material has distinct advantages over polyethylene for the study of diffusionless transformations in molecular solids since direct observation of the interface between the two phases is possible.

We thank the Science Research Council for its support.

References

1. YU. V. MNYUKH and N. N. PETROPAVLOV, *J. Phys. Chem. Solids* **33** (1973) 2079.
2. YU. V. MNYUKH and N. A. PANFILOVA, *ibid* **34** (1973) 159.
3. J. M. THOMAS and J. O. WILLIAMS, *Prog. Solid. State Chem.* **6** (1971) 119.
4. J. O. WILLIAMS, W. JONES, J. P. DESVERGNE, and J. M. THOMAS, *Proc. Roy. Soc.*, to be published.
5. J. W. CHRISTIAN, in "The Mechanism of Phase Transformations in Crystalline Solids" (Institute of Metals, London, 1969).
6. H. KITO, A. PETERLIN, and P. H. GEIL, *J. Appl. Phys.* **35** (1964) 1599.
7. T. SETO, T. HARA, and K. TANAKA, *Japan. J. Appl. Phys.* **7** (1968) 31.
8. P. ALLAN, E. B. CRELLIN, and M. BEVIS, *Phil. Mag.* **27** (1973) 127.
9. M. BEVIS and E. B. CRELLIN, *Polymer* **12** (1971) 666.

Received 16 May
and accepted 21 May 1973.

J. O. WILLIAMS
Edward Davies Chemical Labs.,
University College of Wales,
Aberystwyth, UK

The influence of flaw density and flaw size distribution on the static and dynamic fatigue behaviour of graphite

Graphite is brittle and fractures by the propagation of the most suitably orientated Griffith-type flaw [1]. The material contains a range of flaw sizes and this leads to a large variability in both fracture and fatigue strengths. Fracture strength depends on the distribution of flaws and applied stress and, hence, must also depend on material volume, shape and mode of stressing. Therefore, the design of structural graphite components has to be statistical in nature and must account for flaw distributions etc., to arrive at acceptable probabilities of failure for practical application.

In two recent publications [2, 3] experimental data concerning the fatigue behaviour of graphite have been statistically examined in an effort to develop a practical method of estimating the cumulative fatigue failure probability of brittle materials. This work has prompted us to further consider the effects of flaw density and flaw size distribution on fatigue behaviour. This has been done by comparing the experimental data with the results expected in the case of an imaginary material containing a single flaw. We present here a preliminary and qualitative discussion of our ideas, which we hope will stimulate further discussion and experimental work in this area.

The results presented for RC4 graphite* showed that dynamic fatigue life of this material increases with applied fatigue stress, σ_A, at a

*RC4, extruded graphite from Speer Carbon Co of Canada Ltd, Montreal, Canada.

fixed homologous fatigue stress, Q [2]. The same behaviour was true in the case of static fatigue of this material, although a statistically significant difference between the results at the two values of applied fatigue stress, σ_A, investigated was not demonstrated [3]. Re-examination of the latter results has shown the difference to be statistically significant at the 1% level. Homologous fatigue stress, Q, for a given specimen, is defined as the ratio of the applied fatigue stress, σ_A, to the instantaneous fracture stress, σ_i of that specimen (in references [2] and [3] it was given the notation σ_H).

Consider the hypothetical curves of Fig. 1 in which the relationship between instantaneous fracture stress, σ_i, and fatigue life, tr, is shown for two applied stresses, ${}^L\sigma_A$ and ${}^H\sigma_A$, where ${}^L\sigma_A < {}^H\sigma_A$. Accepting the curve for the lower applied stress, ${}^L\sigma_A$, there are two possible curves for the higher applied stress, ${}^H\sigma_A$, shown as lines 2a and 2b. The difference between 2a and 2b can be more easily appreciated if this information is replotted by replacing the instantaneous fracture stress, σ_i, axis in Fig. 1 with homologous stress, Q, axis (Fig. 2). Effectively, 2a is the experimental result of references [2] and [3] and 2b is the result expected from the imaginary single-flaw material (see below).

At any given value of Q, for the two applied stresses, ${}^H\sigma_A$ and ${}^L\sigma_A$, there are two corresponding values of instantaneous fracture stress, i.e. ${}^H\sigma_i(= {}^H\sigma_A/Q)$ and ${}^L\sigma_i(= {}^L\sigma_A/Q)$, where ${}^H\sigma_i > {}^L\sigma_i$. Therefore, we can consider two specimens, a weak one ($\sigma_i = {}^L\sigma_i$) acted on by the smaller applied stress ${}^L\sigma_A$ and a strong one

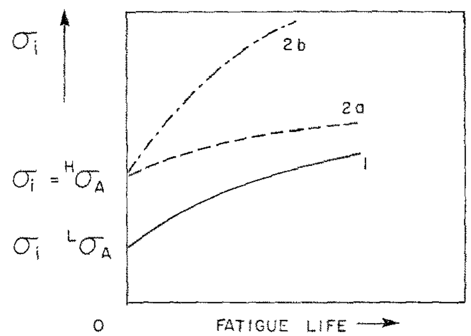

Figure 1 Instantaneous fracture stress versus fatigue life at applied stresses, ${}^L\sigma_A$ and ${}^H\sigma_A$, where ${}^H\sigma_A > {}^L\sigma_A$. Two possible curves for ${}^H\sigma_A$ are shown relative to the assumed ${}^L\sigma_A$ curve. Curve 1 is where $\sigma_A = {}^L\sigma_A$ and curves 2a and b are where $\sigma_A = {}^H\sigma_A$.

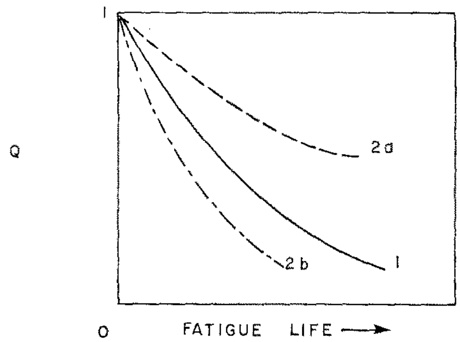

Figure 2 This figure contains the same information as in Fig. 1 except that instantaneous fracture stress has been replaced by homologous stress Q. Curve 1 is where $\sigma_A = {}^L\sigma_A$ and curves 2a and b are where $\sigma_A = {}^H\sigma_A$.

($\sigma_i = {}^H\sigma_i$) acted on by the larger stress, ${}^H\sigma_A$. Assume that for all specimens, it is the propagation of the largest effective flaw that leads to fatigue failure. Assume, also, that effective critical flaw size is inversely proportional to the square of the fracture stress [1]. Then, the fatigue flaw growth distance, x, is proportional to $(\sigma_A^{-2} - \sigma_i^{-2})$, i.e. the difference between the final and original size of the fatigue flaw. Hence, the ratio of fatigue flaw growth distance of the weak and strong specimens is given by:

$$({}^L\sigma_A^{-2} - {}^L\sigma_i^{-2})/({}^H\sigma_A^{-2} - {}^H\sigma_i^{-2})$$

i.e.

$${}^L\sigma_A^{-2}(1 - Q^{-2})/{}^H\sigma_A^{-2}(1 - Q^{-2}) \,.$$

Since the homologous fatigue stress is the same for both specimens, this ratio becomes ${}^L\sigma_A^{-2}/{}^H\sigma_A^{-2}$. The fatigue growth distance, x, must be greater in the weak specimen as this ratio is greater than unity. If the fatigue flaw growth rate of the strong specimen, R_S, is greater than or equal to that for the weak specimen, R_W, the strong specimen will fail first. This is the result one would expect for the imaginary material containing a single flaw (i.e. line 2b in Fig. 2) and it is consistent with the common sense notion that the rate of fatigue flaw growth should increase with applied stress, σ_A (and in this instance also with instantaneous fracture stress, σ_i). The same result is possible even if $R_S < R_W$ and the line 2b (the experimental result) obtains only where

$$R_W > ({}^L\sigma_A^{-2}/{}^H\sigma_A^{-2})\, R_S \,.$$

These results led us to consider the effect of interference of other flaws on the growth of the fatigue flaw to explain the observed fatigue behaviour of RC4 graphite. In the weak specimen the chance of a flaw intersecting or affecting the growth of a fatigue flaw is greater for two reasons, (i) the distance, x, through which the fatigue flaw must grow to reach the critical size for instantaneous propagation is longer in the weak specimen, and (ii) the weak specimen has a greater chance of containing effectively more flaws, which on average will be longer.

Some of the flaws that influence growth of the fatigue flaw will assist its growth by increasing its effective size. Other flaws will blunt the fatigue flaw and retard its growth. It is reasonable to assume that the ratio of the number of flaws which assist to the number of flaws which retard growth of the fatigue flaw will be the same for both weak and strong specimens. If, as is likely, the majority of flaws assist rather than retard fatigue growth, we expect both weak and strong specimens to fail more rapidly than equivalent single-flaw specimens. The chance of premature failure is greater for the weak specimen since, as argued above, the chance of intersecting the growing flaw is greater for this specimen. It is evident too that the weak specimen could fail before the strong one and this would explain the experimental result.

Whether the weak specimen fails before the strong depends on the relative growth rates of their fatigue flaws. The balance between the effect of the faster fatigue flaw propagation rate in the strong specimen and the increased chance of premature failure in the weak specimen, owing to assistance from other flaws, will determine which specimen fails first.

Interaction between the fatigue flaw and other flaws is probable only where the typical distance between flaws is similar or less than the typical fatigue growth distance, x. As Q ranges from zero to unity, there is a range of x values, i.e. a distribution of x. The likelihood of interference between the propagating fatigue flaw and other flaws must be estimated from a knowledge of the distribution of x and the distribution of interflaw distances.

Mercury intrusion porosimetry indicates that the majority of void space in RC4 graphite consists of flaws ranging in effective diameter from 1 to 50 μm. Since the bulk density of RC4 graphite has been measured as ~ 1.7 g cm^{-3}, and assuming the theoretical density is 2.26 g cm^{-3}, it follows that flaws constitute $\sim 24\%$ of the total volume. If the flaws are considered to be spherical and arranged in a simple cubic array, then the distance between nearest neighbouring flaw centres is ~ 1.3 μm for a 1 μm flaw and 65 μm for 50 μm flaws. Therefore the range of flaw free paths is ~ 0.3 to 15 μm. Accepting the approximate nature of this calculation, there is a strong likelihood that interaction will occur between a growing fatigue flaw and another flaw (which may also be growing).

It should be possible, taking the qualitative ideas outlined above, to develop a mathematical model which takes into account the influence of flaw density, flaw shape, and flaw size distribution on the fatigue behaviour of brittle materials.

References

1. A. A. GRIFFITH, *Phil. Trans. Roy. Soc.* **221(A)** **4**, (1920) 163: *Proc. Int. Cong. Appl. Mech. Delft* **1**, (1924) 55.
2. B. J. S. WILKINS "Probability of Failure of Brittle Materials Subjected to Dynamic or Static Fatigue", *J. Materials, JMLSA*, 7 No. 2, June 1972, pp. 251-256.
3. *Idem, J. Amer. Ceram. Soc.* **54** (12) (1971) 593.

Received 5 February
and accepted 24 April 1973

B. J. S. WILKINS
B. F. JONES*
Atomic Energy of Canada Ltd,
Whiteshell Nuclear Research Establishment,
Pinawa, Manitoba, Canada

*Present address: Admiralty Materials Laboratory, Holton Heath, Poole, Dorset, UK.